ChemComm

Cite this: *Chem. Commun.*, 2012, **48**, 4486–4488

www.rsc.org/chemcomm

COMMUNICATION

A dual pH and temperature responsive polymeric fluorescent sensor and its imaging application in living cells†

Liyan Yin, Chunsheng He, Chusen Huang, Weiping Zhu,* Xin Wang, Yufang Xu* and Xuhong Qian*

Received 18th January 2012, Accepted 19th March 2012
DOI: 10.1039/c2cc30404j

A polymeric fluorescent sensor PNME, consisting of A4 and *N*-isopropylacrylamide (NIPAM) units, was synthesized. PNME exhibited dual responses to pH and temperature, and could be used as an intracellular pH sensor for lysosomes imaging. Moreover, it also could sense different temperature change in living cells at 25 and 37 °C, respectively.

The design and development of polymeric fluorescent sensors have garnered a great deal of attention owing to the prompt detection of analytes by fast fluorescence analysis.[1] Because polymeric fluorescent chemosensors are superior to small molecular sensors in terms of stability, easy handling, reuse, signal amplification and so on,[2] they have been intensively used for the detection of cations,[3] molecules,[4] pH[5] and temperature.[6]

Recently, some stimuli-responsive polymers and nanogels have been reported, which have a wide range of applications in optical imaging,[7] biological systems,[8] and analytes detection. There are some dual or multiple stimuli responsive sensors for the detection of oxygen and temperature,[9] oxygen and carbon dioxide,[10] oxygen and pH,[11] pressure and temperature,[12] oxygen, temperature and pH,[13] glucose and temperature,[14] and pH and temperature.[15] However, most of them do not have applications in biological systems, and there is no one dual sensor that can sense intracellular pH and temperature simultaneously.

It is known that polyNIPAM dissolved in water shows a heat-induced phase transition from coiled to globular state, with hydration/dehydration of the polymer chain,[16] which has a polar character at low temperature (coiled state), but an increase in temperature leads to the formation of a less polar domain inside the polymer, associated with its aggregation (globular state). Hence, polyNIPAM exhibits a reversible volume transition in water at approximately 32 °C, defined as the lower critical solution temperature (LCST). The phase transition of the polyNIPAM polymer is reversible, regardless of a heating/cooling process.

State key Laboratory of Bioreactor Engineering, Shanghai Key Laboratory of Chemical Biology, School of Pharmacy, East China University of Science and Technology, 130 Meilong Road, Shanghai, 200237, PR China. E-mail: wpzhu@ecust.edu.cn, yfxu@ecust.edu.cn, xhqian@ecsut.edu.cn; Fax: +86 21-64252603

† Electronic supplementary information (ESI) available. See DOI: 10.1039/c2cc30404j

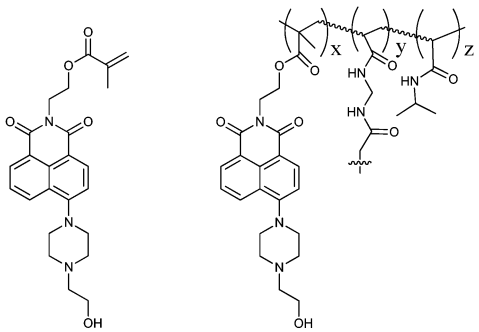

Scheme 1 Chemical structure of **A4** and polymeric fluorescent sensor **PNME**.

Herein, we combine a pH-responsive fluorescent dye with a thermoresponsive polymer to synthesize a novel water soluble polymeric fluorescent sensor **PNME**, which responds to both pH and temperature. **PNME** (Scheme 1) consists of 2-(6-(4-(2-hydroxyethyl)piperazin-1-yl)-1,3-dioxo-1*H*-benzo[*de*] isoquinolin-2(3*H*)-yl)ethyl methacrylate (**A4**) and *N*-isopropylacrylamide (NIPAM) units, which behave as the fluorescent signaling part and the thermo-responsive part, respectively. **PNME** was synthesized by an emulsion polymerization technique using a cross-linker *N*,*N*-methylene-bis-acrylamide (MBAM) and an initiator ammonium persulfate (APS) (Scheme S1, ESI†).

A transmission electron microscopy (TEM) image indicated that **PNME** is roughly spherical in shape (Fig. S1, ESI†), with a diameter of ~50 nm (t > 32 °C), which was further confirmed by dynamic light scattering (DLS) measurements (Fig. S2, ESI†). The ratio (x/y/z) of A4/MBAM/NIPAM units in **PNME** was determined by ^{1}H-NMR ($CDCl_3$, 25 °C) analysis to be 0.7/18.0/81.3 (Fig. S9, ESI†).

Then, we studied the fluorescence response of **PNME** at different pH values and temperatures. **PNME** exhibited a sensitive fluorescence change towards pH between 4.0 and 10.0 at 25 °C (Fig. 1(a) and Fig. S4, ESI†). The fluorescence intensity of **PNME** increased as the pH values decreased. In the acidic pH range, especially pH lower than 4.0, the fluorescence intensity attained its maximum and kept unchanged. In contrast, in the basic pH range up to 10.0, the fluorescence intensity reached its minimum. And the pK_a value of **PNME** was 7.20. The enhancement of fluorescence intensity of **PNME**

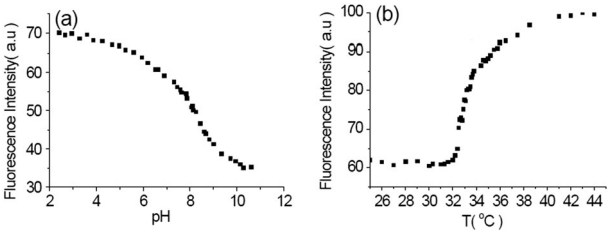

Fig. 1 Fluorescence responses of the polymeric fluorescent sensor **PNME** (7 mg mL^{-1}) to (a) various pH values measured in water at 25 °C and (b) different temperatures at pH 7.08. Excitation wavelength: 410 nm.

was ascribed to the protonation of the amino group in piperazine under acidic conditions, which inhibited the Photo-induced Electron Transfer (PET) process from the amino group to the 1,8-naphthalimide fluorophore. Also, we studied the pH dependence of fluorescence response of **PNME** at different temperatures (Fig. S3, ESI†). The fluorescence intensity of **PNME** increased as the temperature increased.

As shown in Fig. S3(a) (ESI†), the fluorescence intensity of **PNME** in the acidic pH range was stronger than that in the basic pH range at 25 °C, and the fluorescence intensity at 525 nm enhanced by about 2-fold. Similar results were found at 35 °C and 45 °C, but the fluorescence intensity enhanced by about 5-fold (Fig. S3(b) and Fig. S3(c), ESI†).

The fluorescence response of **PNME** to the temperature was firstly observed by heating its aqueous solution at pH 7.08. As shown in Fig. 1(b), the fluorescence intensity of **PNME** kept stable below the lower critical solution temperature (*i.e.*, $t <$ 32 °C), and the fluorescence quantum yield (Φ_F) was 0.018 (in water). While the fluorescence intensity enhanced sharply when the temperature of the **PNME** solution was above 32 °C, and the Φ_F was 0.031 (in water). This was ascribed to the heat-induced phase transition of the polymer's structural change from coiled to globular state, associated with the polarity change of the environment around **PNME**[16,17] (Fig. S8, ESI†). As shown in Fig. S8 (ESI†), the fluorescence intensity of A4 increased when the environment's polarity decreased. We also investigated the temperature dependence of fluorescence response of **PNME** at different pH values (Fig. S5, ESI†). It was interesting that a distinguishable fluorescence change of **PNME** can be observed in the temperature window from 32.5 to 34 °C (Fig. 1(b), and Fig. S6, ESI†). This result also suggested the higher sensitivity of **PNME** to sense temperature changes from 32.5 to 34 °C. The fluorescence enhancement/quenching of **PNME** occurs reversibly. Fig. 2(a) shows the fluorescence intensity change of **PNME**, where the pH is changed repeatedly between 2.55 and 10.70. The result showed that the fluorescence intensity is reversibly changeable at least 10 times. Similarly, when the temperature is changed repeatedly between 28 and 40 °C, the fluorescence intensity of **PNME** showed the identical reversible change with varying temperature, as shown in Fig. 2(b). These results indicated that **PNME** showed a smart structural change in response to the pH and temperature variation, accordingly with a reversible fluorescence response.

Finally, we investigated the fluorescence response of **PNME** to intracellular pH and temperature in the HeLa cells. Generally, cells uptake small particles (<200 nm) such as mesoporous silica nanoparticles (MSNs), polymers and quantum dots through

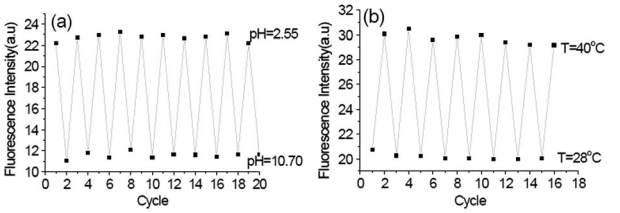

Fig. 2 Change in the fluorescence intensity of the polymeric fluorescent sensor **PNME** (1 mg mL^{-1}) dissolved in water: (a) pH was changed repeatedly between 2.55 and 10.70, (b) temperature was changed repeatedly between 28 and 40 °C.

the endocytosis pathway.[18] Lysosomes are single membrane-bound, small and spherical organelles (in the range of 0.1–1.2 μm in diameter) in the mammalian cells, and they play a principal role in the endocytosis pathway.[19] **PNME** with a diameter of ~50 nm may be endocytosed and is a suitable lysosome-specific probe. Furthermore, the pH in lysosomes (4.5–5.0) is lower than in cytoplasm (~7.4). And the pK_a value of **PNME** was 7.20, with the strong fluorescence at pH < 5.0. These results suggested that **PNME** was likely to accumulate in the acidic lysosomes and expected to be an intracellular sensor for lysosome imaging.

Therefore, we studied the subcellular localization of **PNME** in HeLa cells (Fig. 3). The commercially available lysosome-specific staining probe LysoTracker Red from Molecular Probe was used to co-stain the cells and their colocalizations were conducted. After incubating the cells with **PNME** at 37 °C for 30 minutes, a bright green fluorescence was observed in the HeLa cells under confocal fluorescence microscopy (Fig. 3(a)). The strong green fluorescence of **PNME** can be ascribed to the protonation of the amino group in piperazine in the acidic environment of lysosome, and the green fluorescence was relieved. These results were identical with *in vitro* results (Fig. 1(a)). Then we further studied the subcellular distribution of **PNME** by co-staining cells with a lysosome-specific probe LysoTracker Red. The HeLa cells were first incubated with 5 μM **PNME** at 37 °C for 30 minutes, and then incubated with 100 nM LysoTracker Red at 37 °C for another 30 minutes. As shown in Fig. 3(b), the strong red fluorescence was also visible. These red signals can be attributed to the lysosomal localization of LysoTracker Red. The merged image of green fluorescence of **PNME** and lysosome stained with

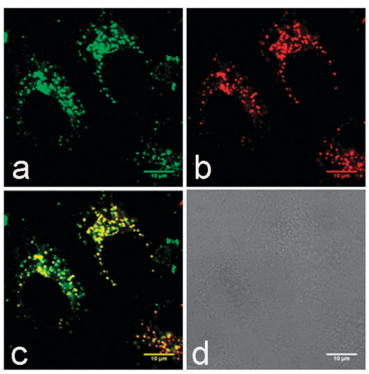

Fig. 3 Confocal fluorescence images of a polymeric fluorescent sensor **PNME** in HeLa cells (a) co-stained with LysoTracker Red (b). (c) is the overlap of (a) and (b), (d) is the bright field image. The bar represents 10 μm.

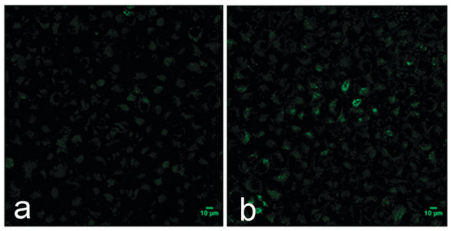

Fig. 4 Confocal fluorescence images of a polymeric fluorescent sensor **PNME** at different temperatures in the HeLa cells: (a) 25 °C and (b) 37 °C, respectively. The bar represents 10 μm.

LysoTracker Red showed convincing yellow fluorescence (Fig. 3(c)), which implied the colocalization of **PNME** in lysosome. Meanwhile, the lysosome localization of **PNME** demonstrated that **PNME** was taken up in lysosomes through the endocytosis pathway and then accumulated in acidic lysosomes (Fig. 3(c)). All these results indicated that **PNME** could be used as an intracellular pH sensor for lysosome imaging in living cells.

The intracellular temperature sensing of **PNME** was also conducted in the HeLa cells through confocal fluorescence microscopy (Fig. 4). As shown in Fig. 4(a), the cells incubated with **PNME** at 25 °C displayed weak green fluorescence, while the cells incubated with **PNME** at 37 °C exhibited brighter green fluorescence, as shown in Fig. 4(b), which was also in good agreement with *in vitro* results (Fig. 1(b)). The result demonstrated that **PNME** could sense the intracellular temperature change in living cells.

In summary, we have synthesized a novel water-soluble polymeric fluorescent sensor **PNME** which responds to both pH and temperature in neutral aqueous solution. **PNME** exhibited a sensitive fluorescence change towards pH between 4.0 and 10.0 at 25 °C, and showed strong fluorescence at pH $<$ 5.0. Meanwhile, the fluorescence intensity of **PNME** increased as the temperature increased, and **PNME** could be used as a thermometer to detect the temperature range from 32 to 40 °C in aqueous solution. The subcellular localization of **PNME** demonstrated that **PNME** with a diameter of $\sim$50 nm could be endocytosed by cells and accumulated in lysosomes, and could be used as an intracellular pH sensor for lysosomes imaging in living cells. Moreover, it also could sense different temperature change in living cells at 25 and 37 °C, respectively.

The authors are grateful for the financial support from the National Natural Science Foundation of China (21076077), the National Science and Technology Pillar Program of China (2011BAE06B02), the National Basic Research Program of China (2010CB126100), the National High Technology Research and Development Program of China (2011AA10A207, 2012AA061601), the Fundamental Research Funds for the Central Universities and the Shanghai Leading Academic Discipline Project (B507). We also wish to thank Mrs Qin Yin for her assistance with confocal fluorescence images.

Notes and references

1 A. P. de Silva, H. Q. N. Gunaratne, T. Gunnlaugsson, A. J. M. Huxley, C. P. McCoy, J. T. Rademacher and T. E. Rice, *Chem. Rev.*, 1997, **97**, 1515.
2 S. W. Thomas, G. D. Joly and T. M. Swager, *Chem. Rev.*, 2007, **107**, 1339.
3 N. J. Li, Q. F. Xu, X. W. Xia, L. H. Wang, J. M. Lu and X. W. Wen, *Mater. Chem. Phys.*, 2009, **114**, 339; J. Lv, C. Ouyang, X. Yin, H. Zheng, Z. Zuo, J. Xu, H. Liu and Y. Li, *Macromol. Rapid Commun.*, 2008, **29**, 1588; H. Lu, Y. Tang, W. Xu, D. Zhang, S. Wang and D. Zhu, *Macromol. Rapid Commun.*, 2008, **29**, 1467; S.-J. Liu, C. Fang, Q. Zhao, Q.-L. Fan and W. Huang, *Macromol. Rapid Commun.*, 2008, **29**, 1212; F. Vogtle, S. Gestermann, C. Kauffmann, P. Ceroni, V. Vicinelli and V. Balzani, *J. Am. Chem. Soc.*, 2000, **122**, 10398.
4 C. Xing, M. Yu, S. Wang, Z. Shi, Y. Li and D. Zhu, *Macromol. Rapid Commun.*, 2007, **28**, 241.
5 Y. Q. Tian, F. Y. Su, W. Weber, V. Nandakumar, B. R. Shumway, Y. G. Jin, X. F. Zhou, M. R. Holl, R. H. Johnson and D. R. Meldrum, *Biomaterials*, 2010, **31**, 7411; H. S. Peng, J. A. Stolwijk, L. N. Sun, J. Wegener and O. S. Wolfbeis, *Angew. Chem., Int. Ed.*, 2010, **49**, 4246; S. Uchiyama and Y. Makino, *Chem. Commun.*, 2009, 2646.
6 F. Vetrone, R. Naccache, A. Zamarron, A. J. de la Fuente, F. Sanz-Rodriguez, L. M. Maestro, E. M. Rodriguez, D. Jaque, J. G. Sole and J. A. Capobianco, *ACS Nano*, 2010, **4**, 3254; Y. Shiraishi, R. Miyamoto and T. Hirai, *Org. Lett.*, 2009, **11**, 1571; C. Gota, K. Okabe, T. Funatsu, Y. Harada and S. Uchiyama, *J. Am. Chem. Soc.*, 2009, **131**, 2766; T. Barilero, T. Le Saux, C. Gosse and L. Jullien, *Anal. Chem.*, 2009, **81**, 7988; C. Gota, S. Uchiyama and T. Ohwada, *Analyst*, 2007, **132**, 121; K. Iwai, Y. Matsumura, S. Uchiyama and A. P. de Silva, *J. Mater. Chem.*, 2005, **15**, 2796.
7 T. Hasegawa, Y. Kondo, Y. Koizumi, T. Sugiyama, A. Takeda, S. Ito and F. Hamada, *Bioorg. Med. Chem.*, 2009, **17**, 6015; C. Koopmans and H. Ritter, *J. Am. Chem. Soc.*, 2007, **129**, 3502.
8 M. Yan, Z. Liu, D. Lu and Z. Liu, *Biomacromolecules*, 2007, **8**, 560; M. Yan, J. Ge, Z. Liu and P. Ouyang, *J. Am. Chem. Soc.*, 2006, **128**, 11008.
9 S. M. Borisov and O. S. Wolfbeis, *Anal. Chem.*, 2006, **78**, 5094.
10 S. M. Borisov, R. Seifner and I. Klimant, *Anal. Bioanal. Chem.*, 2011, **400**, 2463; S. M. Borisov, C. Krause, S. Arain and O. S. Wolfbeis, *Adv. Mater.*, 2006, **18**, 1511.
11 N. B. Borchert, G. V. Ponomarev, J. P. Kerry and D. B. Papkovsky, *Anal. Chem.*, 2011, **83**, 18; K. Schneider, V. Schutz, G. T. John and E. Heinzle, *Bioprocess Biosyst. Eng.*, 2010, **33**, 541; G. Mistlberger, K. Koren, S. M. Borisov and I. Klimant, *Anal. Chem.*, 2010, **82**, 2124; G. S. Vasylevska, S. M. Borisov, C. Krause and O. S. Wolfbeis, *Chem. Mater.*, 2006, **18**, 4609.
12 M. I. J. Stich, S. Nagl, O. S. Wolfbeis, U. Henne and M. Schaeferling, *Adv. Funct. Mater.*, 2008, **18**, 1399.
13 M. I. J. Stich, M. Schaeferling and O. S. Wolfbeis, *Adv. Mater.*, 2009, **21**, 2216.
14 D. Wang, T. Liu, J. Yin and S. Liu, *Macromolecules*, 2011, **44**, 2282.
15 A. Saha, S. Manna and A. K. Nandi, *Soft Matter*, 2009, **5**, 3992; C. Pietsch, R. Hoogenboom and U. S. Schubert, *Angew. Chem., Int. Ed.*, 2009, **48**, 5653; G. Pasparakis, M. Vamvakaki, N. Krasnogor and C. Alexander, *Soft Matter*, 2009, **5**, 3839; J.-J. Lin and Y.-C. Hsu, *J. Colloid Interface Sci.*, 2009, **336**, 82; Y.-Y. Li, H. Cheng, J.-L. Zhu, L. Yuan, Y. Dai, S.-X. Cheng, X.-Z. Zhang and R.-X. Zhuo, *Adv. Mater.*, 2009, **21**, 2402; H. Kobayashi, *Anal. Sci.*, 2009, **25**, 1043; S. Uchiyama, N. Kawai, A. P. de Silva and K. Iwai, *J. Am. Chem. Soc.*, 2004, **126**, 3032.
16 Y. Katsumoto, T. Tanaka, H. Sato and Y. Ozaki, *J. Phys. Chem. A*, 2001, **106**, 3429.
17 D. P. Wang, R. Miyamoto, Y. Shiraishi and T. Hirai, *Langmuir*, 2009, **25**, 13176.
18 J. L. Vivero-Escoto, I. I. Slowing, B. G. Trewyn and V. S. Y. Lin, *Small*, 2010, **6**, 1952; Y. Shiraishi, R. Miyamoto and T. Hirai, *J. Photochem. Photobiol., A*, 2008, **200**, 432.
19 I. M. Stuart Kornfeld, *Annu. Rev. Cell Biol.*, 1989, **5**, 483; R. W. Christian de Duve, *Annu. Rev. Physiol.*, 1966, **28**, 435.

